NeuroImage: Clinical 24 (2019) 101970

Contents lists available at ScienceDirect

NeuroImage: Clinical

journal homepage: www.elsevier.com/locate/ynicl

Resting-state fMRI dynamic functional network connectivity and associations with psychopathy traits

Flor A. Espinoza[a,h,*,1], Nathaniel E. Anderson[a,1], Victor M. Vergara[a,h], Carla L. Harenski[a], Jean Decety[b,g], Srinivas Rachakonda[a,h], Eswar Damaraju[a,h], Michael Koenigs[c], David S. Kosson[d], Keith Harenski[a], Vince D. Calhoun[a,e,h,2], Kent A. Kiehl[a,f,2]

[a] The Mind Research Network, Albuquerque, NM, USA
[b] Department of Psychology, University of Chicago, Chicago, IL, USA
[c] Department of Psychiatry, University of Wisconsin Madison, Madison, WI, USA
[d] Department of Psychology, Rosalind Franklin University of Medicine and Science, Chicago, IL, USA
[e] Department of Electrical and Computer Engineering, University of New Mexico, Albuquerque, NM, USA
[f] Department of Psychology, University of New Mexico, Albuquerque, NM, USA
[g] Departments of Psychiatry and Behavioral Neuroscience, University of Chicago, Chicago, IL, USA
[h] Tri-institutional Center for Translational Research in Neuroimaging and Data Science (TReNDS), Georgia State University, Georgia Institute of Technology, and Emory University, Atlanta, GA, USA

ARTICLE INFO

Keywords:
Psychopathy
Resting-state fMRI
Dynamic functional network connectivity
Group independent component analysis
K-means clustering

ABSTRACT

Studies have used resting-state functional magnetic resonance imaging (rs-fMRI) to examine associations between psychopathy and brain connectivity in selected regions of interest as well as networks covering the whole-brain. One of the limitations of these approaches is that brain connectivity is modeled as a constant state through the scan duration. To address this limitation, we apply group independent component analysis (GICA) and dynamic functional network connectivity (dFNC) analysis to uncover whole-brain, time-varying functional network connectivity (FNC) states in a large forensic sample. We then examined relationships between psychopathic traits (PCL-R total scores, Factor 1 and Factor 2 scores) and FNC states obtained from dFNC analysis. FNC over the scan duration was better represented by five states rather than one state previously shown in static FNC analysis. Consistent with prior findings, psychopathy was associated with networks from paralimbic regions (amygdala and insula). In addition, whole-brain FNC identified 15 networks from nine functional domains (subcortical, auditory, sensorimotor, cerebellar, visual, salience, default mode network, executive control and attentional) related to psychopathy traits (Factor 1 and PCL-R scores). Results also showed that individuals with higher Factor 1 scores (affective and interpersonal traits) spend more time in a state with weaker connectivity overall, and changed states less frequently compared to those with lower Factor 1 scores. On the other hand, individuals with higher Factor 2 scores (impulsive and antisocial behaviors) showed more dynamism (changes to and from different states) than those with lower scores.

1. Introduction

Psychopathy is a personality disorder associated with a combination of affective, interpersonal, lifestyle, and behavioral features. These prominently include grandiosity, a lack of remorse and empathy, irresponsibility, and poor behavioral controls (Hare, 2003). Psychopathy is known to affect < 1% of the general population, but 15% to 20% of incarcerated offenders (Hare, 2003). Incarcerated individuals with psychopathy who are released from prison have higher recidivism rates than those showing less psychopathic traits (Hemphill et al., 1998).

Mounting evidence suggests organic neurodevelopmental origins for psychopathy (Gao et al., 2009). However, our understanding of its pathogenesis remains incomplete. Structural and functional MRI studies have provided evidence showing that psychopathy is related to

* Corresponding author at: The Mind Research Network, Albuquerque, NM, USA; Tri-institutional Center for Translational Research in Neuroimaging and Data Science (TReNDS), Georgia State University, Georgia Institute of Technology, and Emory University, Atlanta, GA, USA.
E-mail address: fespinoza@mrn.org (F.A. Espinoza).
[1] Co-authors with equally contribution to this work.
[2] Senior authors who equally contributed to this work.

https://doi.org/10.1016/j.nicl.2019.101970
Received 14 February 2019; Received in revised form 25 July 2019; Accepted 3 August 2019
Available online 05 August 2019

abnormalities in limbic and paralimbic regions (Anderson and Kiehl, 2012; Ermer et al., 2012; Kiehl, 2006), which are important for integrating emotional information into higher order cognitive processing. Traditional neurocognitive models of psychopathy highlight brain regions such as the amygdala and ventromedial prefrontal cortex, citing their roles in guiding decision-making and behavior based on emotional cues and value representation (Blair, 2008; Hiser and Koenigs, 2018). Other models have stressed the fundamental role of attention in guiding what information is salient and further integrated into ongoing behavioral management strategies (Newman, 1998; Newman et al., 2010). These attention-based models implicate a wide array of brain regions, stressing impaired integration across a number of large-scale intrinsic networks in the brain (Anderson et al., 2018; Hamilton et al., 2015).

Measures of brain functional connectivity are important for understanding psychopathy as they may provide additional insight about deficits in brain information processing architecture that precipitate psychopathic traits. A small subset of psychopathy studies have focused directly on the examination of abnormalities in brain connectivity associated with psychopathic traits (Espinoza et al., 2018; Hoppenbrouwers et al., 2013; Juarez et al., 2013; Kiehl, 2006; Korponay et al., 2017a; Korponay et al., 2017b; Motzkin et al., 2011; Philippi et al., 2015; Raine et al., 2003; Wolf et al., 2015; Yoder et al., 2015). These studies document disrupted connectivity across a wide range of brain regions, prominently including limbic and paralimbic areas, but also involving connectivity between limbic areas and extralimbic nodes such as parietal association cortex, occipital cortex, and sensorimotor areas. Together, this suggests, even if neural abnormalities associated with psychopathy primarily affect paralimbic areas, neural communication also appears to be affected across more widely distributed brain areas. Moreover, the functional connectivity studies to date have only examined psychopathy using static connectivity, without considering changes of connectivity across time. To address this limitation, using a large sample of resting state fMRI data formed mostly by incarcerated males, we examined for whole-brain, time-varying functional network connectivity (FNC) states across time, and assessed for relationship between psychopathic traits and FNC states.

Dynamic functional network connectivity (dFNC) is an extension of static FNC analysis that takes into account fluctuating states of connectivity, within subjects, across the time domain (Allen et al., 2014). These fluctuations can provide additional valuable information about individual differences in information processing and encoding of cognitive events. We hypothesized that by analyzing time-varying resting state FNC in the whole brain, we can uncover connectivity states obscured in traditional static connectivity analysis, and further, we can identify networks both within and outside limbic/paralimbic regions associated with psychopathic traits not revealed by seed or region of interest analysis. By identifying time-varying patterns in network connectivity associated with psychopathy, we hope to illuminate the extent to which these network dynamics are impaired in psychopathy, and further clarify what specific neural systems contribute to these pathological traits.

2. Methods

2.1. Participants

Resting-state fMRI data were collected from 985 male participants (903 prison inmates and 82 community healthy controls). All participants were scanned with the Mind Research Network's 1.5 T mobile scanner. Inmates were located at one of eight prisons in New Mexico or Wisconsin where we have established research programs. Participant age range was from 19 to 63 (average age = 33.7 years, SD = 9 years). Participants' demographics are shown in Table 1.

Table 1
Participants' information.

	Mean	SD	Min.	Max.
PCL-R total scores	22.2	7.2	3.2	40
Factor 1 scores	7.3	3.7	0	16
Factor 2 scores	12.7	3.8	2	20
Age (years)	33.7	9.1	19	63
IQ	97	13.4	66	137

2.2. Psychopathy scores

Participants were assessed for psychopathy with the Hare Psychopathy Checklist-Revised (PCL-R) (Hare, 1991). The PCL-R is considered to be the most accepted measure for assessing psychopathy in forensic samples (Kiehl, 2006). The PCL-R consists of 20 items which are scored on a three-point scale, 0 (does not apply), 1 (applies somewhat), and 2 (definitely applies). It is based on participants' clinical interview and extensive file review conducted by trained Research Assistants. The resulting PCL-R total scores range from 0 to 40. Factor analyses of the 20 PCL-R items have revealed two correlated factors. Factor 1 scores correspond to affective/interpersonal characteristics, whereas Factor 2 scores correspond to impulsive, nomadic lifestyle and early and persistent antisocial behavior (Hare and Neumann, 2010; Harpur et al., 1989). The PCL-R scores for this group ranged from 3.2 to 40 (mean = 22.2 and standard deviation = 6.5). Participants' PCL-R, Factors 1 and 2 scores are shown in Table 1. A total of one hundred sixty-seven inmates have PCL-R scores equal to or larger than the traditional clinical cutoff of 30 to be classified as psychopathic; this cutoff was used for the categorical analyses. Psychopathic traits are also commonly examined as dimensional measures, defined by individual factor scores on the PCL-R (Hare and Neumann, 2005). For dimensional analysis, PCL-R Factor 1 and Factor 2 scores were treated as continuous variables and correlated to the rs-fMRI data. The study was approved by the Ethical and Independent Review Services (IRB) and all participants provided written informed consent. Participants were paid at a rate commensurate with institution compensation for work assignments at their facility.

2.3. Imaging parameters

Resting-state fMRI images were collected on prison grounds using a mobile Siemens 1.5 T Avanto with advanced SQ gradients (max slew rate 200 T/m/s, 346 T/m/s vector summation, rise time 200 us) equipped with a 12-element head coil. The EPI gradient-echo pulse sequence (TR = 2000 ms, TE = 39 ms, flip angle 90°, FOV 24 × 24 cm, 64 × 64 matrix, 3.4 × 3.4 mm in-plane resolution, 4 mm slice thickness, 1 mm gap, 30 slices) effectively covered the entire brain (150 mm) in 2.0 s. Head motion was minimized using padding and restraint. The participants were asked to lay still, look at the fixation cross and keep eyes open during the five minute resting state fMRI scanning. Compliance with instructions was monitored by eye tracking.

2.4. EPI preprocessing

Data were pre-processed using statistical parametric mapping (Friston et al., 1994) (http://www.fil.ion.ucl.ac.uk/spm) including slice-timing correction, realignment (INRIalign), co-registration, and spatial normalization, and then transformed to the Montreal Neurological Institute standard space at a resolution of a $3 \times 3 \times 3\,mm^3$. Despiking consisted of the orthogonalization with respect to spike regressors. Each spike is represented by an independent regressor valued one at the spike time point and zero everywhere else. The DVARS method (Power et al., 2012) was used to find spike regressors where the root mean square exceeded three standard deviations. Time-courses were also orthogonalized with respect to the following: (1) linear,

quadratic, and cubic trends; (2) the six realignment parameters; (3) realignment parameters derivatives; and (4) spike regressors. A full width half maximum Gaussian kernel of 6 mm was then used for spatial smoothing.

2.5. Group independent component analysis

We applied group independent component analysis (GICA) on the preprocessed data using the GIFT toolbox (http://mialab.mrn.org/software/gift) (Calhoun et al., 2001). The rs-fMRI data were compressed using two stages of principal component analysis (PCA) (Rachakonda et al., 2016). For the first data reduction we retained 100 principal components (PCs). Based on previously published work (Allen et al., 2011), we chose to retain 75 independent components (ICs) for group data reduction (Erhardt et al., 2011). Individual specific spatial maps and their time-courses were obtained using GICA. Out of the 75 ICs that were estimated, 55 components were identified as components of resting state networks (RSNs) by evaluating the high to low frequency power in the spectra of components, as well as whether peak activations took place in gray matter (Allen et al., 2011; Meda et al., 2008; Robinson et al., 2009). The other twenty components were excluded as they appeared to be related to motion artifacts or the spatial maps including white matter, the ventricular system, or cerebral spinal fluid, or had irregular time course spectra power (Allen et al., 2011). The time-courses of the RSNs underwent despiking and band-pass by filtering with [0.01 0.15] Hz cutoffs. In addition, to reduce motion effects in the analysis, the movement parameters (translation and rotation) and their derivatives were regressed out of the RSNs time-courses at the individual level. Since in this study we wanted to focus on abnormalities in inmates dFNC associated with psychopathy traits, the eighty-two community healthy controls participants were exclude from the rest of the analysis. In addition, we also excluded seventy-nine inmates (seventy-six who did not complete the PCL-R scores and three with PCL-YV scores), leaving a total number of 824 participants in the remaining of the study.

2.6. Dynamic functional network connectivity (dFNC)

Dynamic FNC analysis exposes time-varying patterns of FNC within subjects over scan duration. To estimate these patterns, the time-courses for the selected number of RSNs (NRSNs = 55) are discretized into sequences of overlapping time domains using the tapered sliding window approach (Allen et al., 2014; Sakoglu et al., 2010). For each subject, 126 time-windowed domains were obtained for each of the RSNs' time-courses by convolving a rectangular window width of 15 TRs (=30 s, TR = 2 s) with a Gaussian of sigma 3 TRs, and sliding in 1 TR step. Next, in each time-windowed domain, FNC was computed as the pairwise correlation between windowed RSNs time-courses. A total of 1485 [= NRSNs * (NRSNs - 1) / 2] unique FNC pairs measuring time-windowed connectivity were obtained. Then, a symmetric matrix was formed with the FNC pairs as a representation of the subject's FNC in that time-windowed domain. Overall, we created a total of 103,824 windowed FNC (wFNC) matrices (=824 participants times 126 wFNC) which form the dFNC data. To improve the estimation of correlations among time-courses with short time domain, the graphical LASSO algorithm (Friedman et al., 2008) was used to estimate covariance matrices from regularized precision matrices or inverse covariance matrices (Smith et al., 2011). A penalty on the L1 norm of the precision matrix was applied to enforce sparsity. The regularization parameter was optimized for each subject by evaluating the log-likehood of unseen data (subject's covariance matrices) in a cross-validation framework. The estimated wFNC also referred to as dFNC matrices represent the changes in covariance (correlation) between RSNs as a function of time. The dFNC matrices were Fisher-transformed to stabilize variance before performing statistical analysis.

2.7. Clustering analysis of dFNC

Clustering analysis applied to all subjects' dFNC data allows the identification of occurring and reoccurring FNC states during scan duration. This approach was adopted based on previous dFNC work that has validated the application of these clustering approaches to this kind of data (Allen et al., 2014; Calhoun et al., 2014; Hutchison et al., 2013). Clustering analysis was performed using k-means algorithm with the L1 distance (Manhattan distance). The optimal number of clusters K = 5 was obtained using the elbow criterion applied to a cluster index computed from running k-means on all subjects' dFNC data with the number of clusters ranging from two to eight. The cluster index was defined as the ratio of the within-cluster sum distances to the between-cluster sum distances. The clustering results (clusters and output metrics) are reported for the optimal number of clusters. The five clusters referred to as FNC states described five connectivity patterns that individual subjects move between over time. The total number of dFNC and individuals per state was also obtained. It is important to note that not all individuals have dFNC in all states. Therefore the number of individuals in each state is a subset of the entire subject cohort. The three output metrics which provide clustering measures are mean dwell time (average time an individual spends in each state before changing to another state), fraction time (percentage of total time an individual spends in each state), and number of transitions (changes between states).

2.8. Statistical analyses

Dynamic FNC data analysis was broken into two parts, examining continuous and discrete psychopathy scores. In the continuous case, all subjects ($N = 824$) were included. In the discrete case, PCL-R was discretized to form two groups close in sizes and well differentiated, non-PSY (PCL-$R \leq 15$, $N = 159$) and PSY (PCL-$R \geq 30$, $N = 167$). Regression analysis, with PCL-R total scores (model 1) and Factors 1 and Factor 2 scores (model 2) as main covariates, and age, IQ, and motion parameters as nuisance covariates was performed to identify associations between psychopathy and states FNC, and clustering measures [mean dwell time (MDT), fraction time (FT) spend in each state, number of transitions (NT) between states]. For each participant, the translation and rotation parameters were computed as the mean of the sums of the absolute translation and rotation frame displacements. All presented results were corrected for multiple testing at significant level < 0.05.

3. Results

3.1. Group independent component analysis

Based on their anatomical, functional properties, neurosynth labeling (http://neurosynth.org/), and similarities to other RSNs found on previous rs-fMRI studies (Allen et al., 2011; Smith et al., 2009), the selected fifty-five RSNs were grouped into nine functional domains: subcortical (SBC), auditory (AUD), sensorimotor (SEN), cerebellar (CER), visual (VIS), salience (SAL), default mode network (DMN), executive control (ECN), and attentional (ATT). Fig. 1 shows the spatial maps of the 55 selected RSNs grouped by functional domains. Table 2 presents the 55 RSNs along with their IC number, name description and peak activation coordinates (x, y and z).

3.2. Dynamic functional network connectivity

Time-varying FNC over the scan duration can be represented by 5 states (Fig. 2) rather than the single state shown in (Espinoza et al., 2018). State-1 (15% dFNC) shows pronounced anticorrelations between RSNs from the default mode network domain and other domains. This state also shows strong positive correlations within RSNs from the

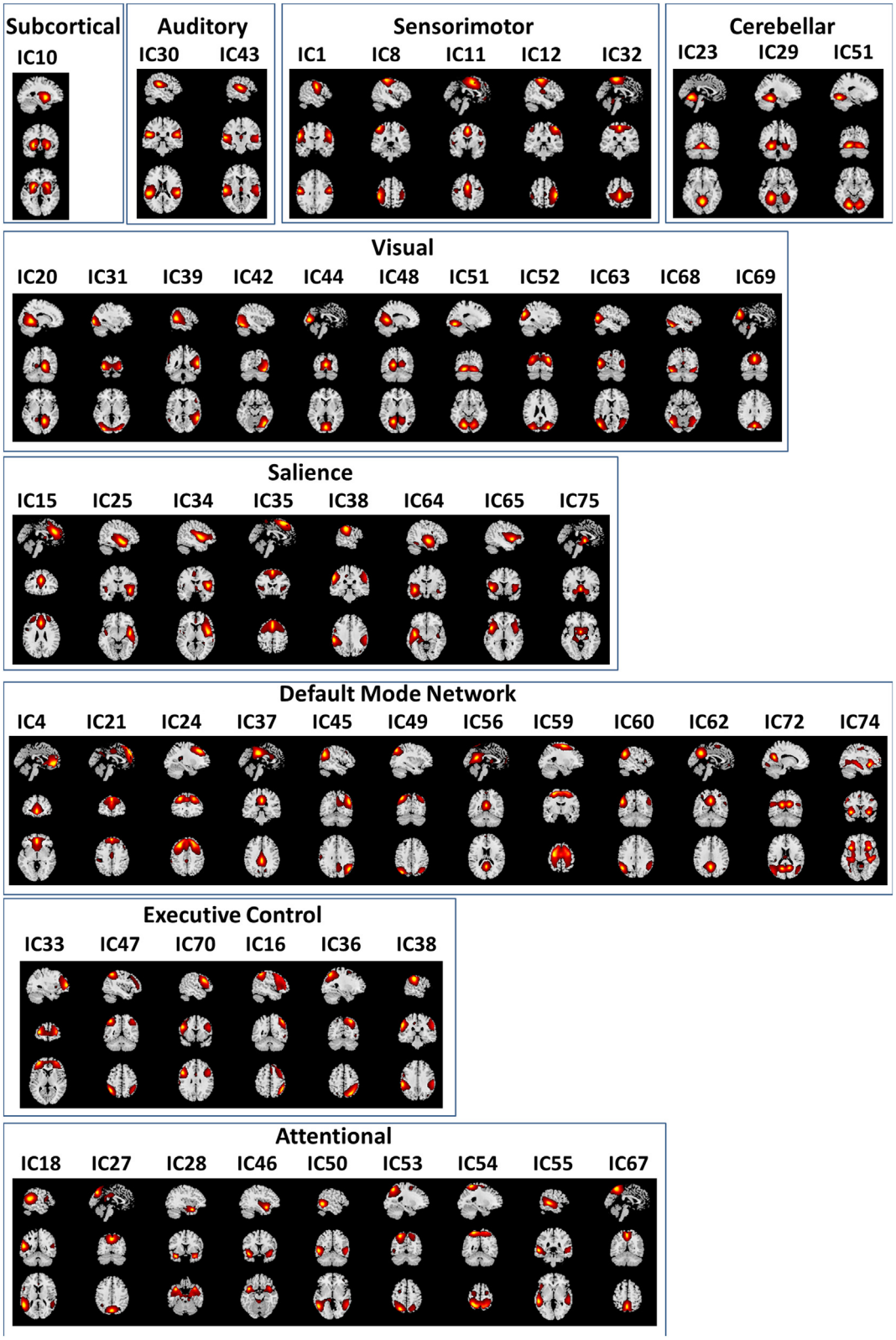

Fig. 1. Spatial maps of the 55 independent components identified as resting state networks (RSNs), grouped into nine domains based on their anatomical and functional properties: subcortical (SBC), auditory (AUD), sensorimotor (SEN), cerebellar (CER), visual (VIS), salience (SAL), default mode network (DMN), executive control (ECC), and attentional (ATT).

sensorimotor, visual default mode network, executive control, and attentional domains. State-2 (7% dFNC), shows mostly positive correlations among RSNs from all domains. State-3 (18% dFNC) is similar to State-1 with weaker positive correlations within and between domains. State-4 (22% dFNC) shows weak connectivity among RSNs. State-5, occurring with the highest frequency (39% dFNC), is similar to states 1 and 3 with weaker connectivity between default mode networks and the rest of RSNs.

Table 2
Resting state networks (RSNs) ICs numbers, domain names and MNI peak coordinates.

ICs numbers and RSNs domain names	ICs, domains
Subcortical (SBC)	
IC10: putamen	(−26.5, 3.5, −2.5)
Auditory (AUD)	
IC30: superior temporal gyrus	(−57.5, −20.5, 8.5)
IC43: postcentral gyrus	(−50.5, −30.5, 18.5)
Sensorimotor (SEN)	
IC35: supplementary motor area	(0.5, 23.5, 56.5)
IC32: paracentral lobule	(0.5, −30.5, 60.5)
IC8: left postcentral gyrus	(−44.5, −35.5, 59.5)
IC12: right postcentral gyrus	(45.5, −32.5, 59.5)
IC1: precentral gyrus	(−54.5, −9.5, 30.5)
IC11: supplementary motor area	(0.5, 2.5, 50.5)
Cerebellar (CER)	
IC23: cerebellum	(−0.5, −62.5, −12.5)
IC29: cerebellum lobule VI	(−24.5, −45.5, −15.5)
IC51: bilateral cerebellum lobule VI	(−18.5, −74.5, −14.5)
Visual (VIS)	
IC44: cuneus	(0.5, −83.5, 3.5)
IC20: right lingual gyrus	(15.5, −54.5, −2.5)
IC48: left lingual gyrus	(−15.5, −59.5, 3.5)
IC52: superior occipital gyrus	(33.5, −81.5, 24.5)
IC68: fusiform gyrus	(−47.5, −62.5, −18.5)
IC69: cuneus	(0.5, −77.5, 29.5)
IC42: right inferior occipital gyrus	(41.5, −71.5, −17.5)
IC31: middle occipital gyrus	(−32.5, −90.5, −2.5)
IC63: left middle occipital gyrus	(−47.5, −72.5, 11.5)
IC39: superior temporal gyrus (STG)	(59.5, −45.5, 9.5)
Salience (SAL)	
IC75: amygdala	(0.5, −2.5, −6.5)
IC15: anterior cingulate cortex	(0.5, 30.5, 26.5)
IC34: operculum/insula	(47.5, −2.5, 6.5)
IC65: insula	(−45.5, 14.5, −3.5)
Default Mode Network (DMN)	
IC45: right angular gyrus	(50.5, −63.5, 30.5)
IC49: angular gyrus	(−35.5, −74.5, 44.5)
IC56: posterior cingulate cortex	(0.5, −54.5, 17.5)
IC60: angular	(−50.5, −59.5,30.5)
IC62: precuneus / posterior cingulate cortex	(−0.5, −56.5, 33.5)
IC72: posterior cingulate cortex	(−14.5, −60.5, 18.5)
IC4: anterior cingulate cortex	(−0.5, 45.5, −5.5)
IC21: medial prefrontal cortex	(0.5, 50.5, 41.5)
IC24: middle frontal gyrus	(−24.5, 32.5, 42.5)
IC37: posterior cingulate gyrus	(0.5, −30.5, 33.5)
IC74: anterior cingulate cortex	(−35.5, 17.5, −9.5)
IC59: middle frontal gyrus	(−26.5, −6.5, 62.5)
Executive Control (ECN)	
IC33: orbital frontal cortex	(−32.5, 56.5, 6.5)
IC47: inferior parietal lobule	(−42.5, −54.5, 53.5)
IC70: middle frontal gyrus	(−51.5, 14.5, 29.5)
IC16: inferior parietal lobule	(47.5, −51.5, 53.5)
IC36: superior parietal lobule	(29.5,-68.5,53.5)
IC38: left inferior parietal lobule	(−59.5, −29.5, 35.5)
Attentional (ATT)	
IC27: cuneus	(0.5, −74.5, 41.5)
IC67: precuneus	(0.5, −59.5, 56.5)
IC53: superior parietal lobule	(−23.5, −68.5, 53.5)
IC54: superior parietal lobule	(−24.5, −51.5, 65.5)
IC25: superior temporal gyrus	(44.5, −5.5, −11.5)
IC64: superior temporal gyrus	(−42.5, −11.5, −9.5)
IC18: left middle temporal gyrus	(−54.5, −50.5, 12.5)
IC55: middle temporal gyrus	(−57.5, −35.5, −2.5)
IC28: temporal pole / superior temporal gyrus	(−38.5, 9.5, −26.5)
IC46: temporal pole / superior temporal gyrus	(−39.5, 9.5, −18.5)
IC50: middle temporal gyrus	(−54.5, −57.5, −3.5)

3.2.1. Continuous psychopathy scores (all subjects)

In State-3 we identified negative associations between the FNC pair insula - precentral gyrus and Factor-1 scores (Fig. 3a). The connectivity between insula and precentral gyrus decreases as Factor 1 scores increases. In State-4, we identified positive (two) and negative (six) associations between FNC pairs and Factor 1 scores (Fig. 3b). Factor 1 scores are positively correlated with connectivity between the FNC pairs: (1) middle frontal gyrus and cerebellum, (2) precuneus and putamen. Factor 1 scores are negatively correlated with connectivity between the FNC pairs (1) amygdala and superior temporal gyrus, (2) insula and supplementary motor area, (3) superior temporal gyrus and superior occipital gyrus, (4–6) middle temporal gyrus and postcentral gyrus, supplementary motor and superior occipital gyrus. The beta- and p- values from the linear regression models are listed in Table 3. No significant associations between states FNC and continuous PCL-R and Factor 2 scores were found.

Associations between clustering measures and psychopathy scores: In State-5, we identified positive association between mean dwell time and Factor 1 scores (p-value = .0065, beta = 0.5480), on average subjects with higher Factor 1 scores spend more time in State-5. In addition, we identified negative association between number of transitions and Factor 1 scores (p-value = .0178, beta = −0.0803), and positive associations with Factor 2 (p-value = .0360, beta = 0.0684) scores. Subjects with higher Factor 1 scores change states less often, while subjects with higher Factor 2 scores change states more often. No significant associations between clustering measures and PCL-R scores were found.

3.2.2. Discrete psychopathy scores (two groups, non-PSY (PCL-R ≤ 15, Group-1) and PSY (PCL-R ≥ 30, Group-2)

In State-5, we found group differences between three FNC pairs and PCL-R scores (Fig. 4). Compared to non-PSY, PSY subjects have lower connectivity between the FNC pairs: amygdala and left/right lingual gyrus, superior occipital gyrus. The p and beta values are listed in Table 3. None of the clustering measures showed significant differences between the non-PSY and PSY groups.

4. Discussion

This study examined dynamic states of functional network connectivity observed during task-free, resting-state scans, and related differential patterns of connectivity to psychopathic personality traits measured in an incarcerated sample. We observed several significant differences in dynamic connectivity measures attributable to individual factor elements of psychopathy, as well unique patterns attributable, categorically, to those meeting full diagnostic criteria for psychopathy. These findings support recent examples of disrupted functional connectivity in psychopathy (Espinoza et al., 2018; Juarez et al., 2013; Motzkin et al., 2011; Philippi et al., 2015), but add more specificity with regard to transitioning states of connectivity in the resting-state. The present findings are highly relevant for progressing our understanding of the neurocognitive abnormalities giving rise to psychopathy, especially within the context of recent models that describe irregularities in attentional processes and fundamental integrative deficits across intrinsic networks in the brain (Hamilton et al., 2015). These results further reinforce a growing body of literature demonstrating the importance of dynamic shifts in network connectivity for understanding cognitive abnormalities associated with various domains of psychopathology and mental health.

Examining continuous scores on psychopathy, several prominent negative associations between the interpersonal/affective dimension (Factor 1) of psychopathy and connectivity were evident in dynamic states 3 and 4. These included FNC pairs between paralimbic regions (e.g. amygdala and insula) extending to extra-limbic functional nodes (e.g. sensorimotor, supplementary motor, occipital). These results reflect similar aberrations in static functional connectivity involving the insula, amygdala, sensorimotor, and visual nodes observed in the static analysis of this rs-fMRI data (Espinoza et al., 2018). The present findings further confirm that well-established functional abnormalities in limbic/paralimbic regions associated with psychopathy have extended effects that disrupt the strength of neural signals across large-scale networks outside paralimbic areas, also described in Espinoza et al.,

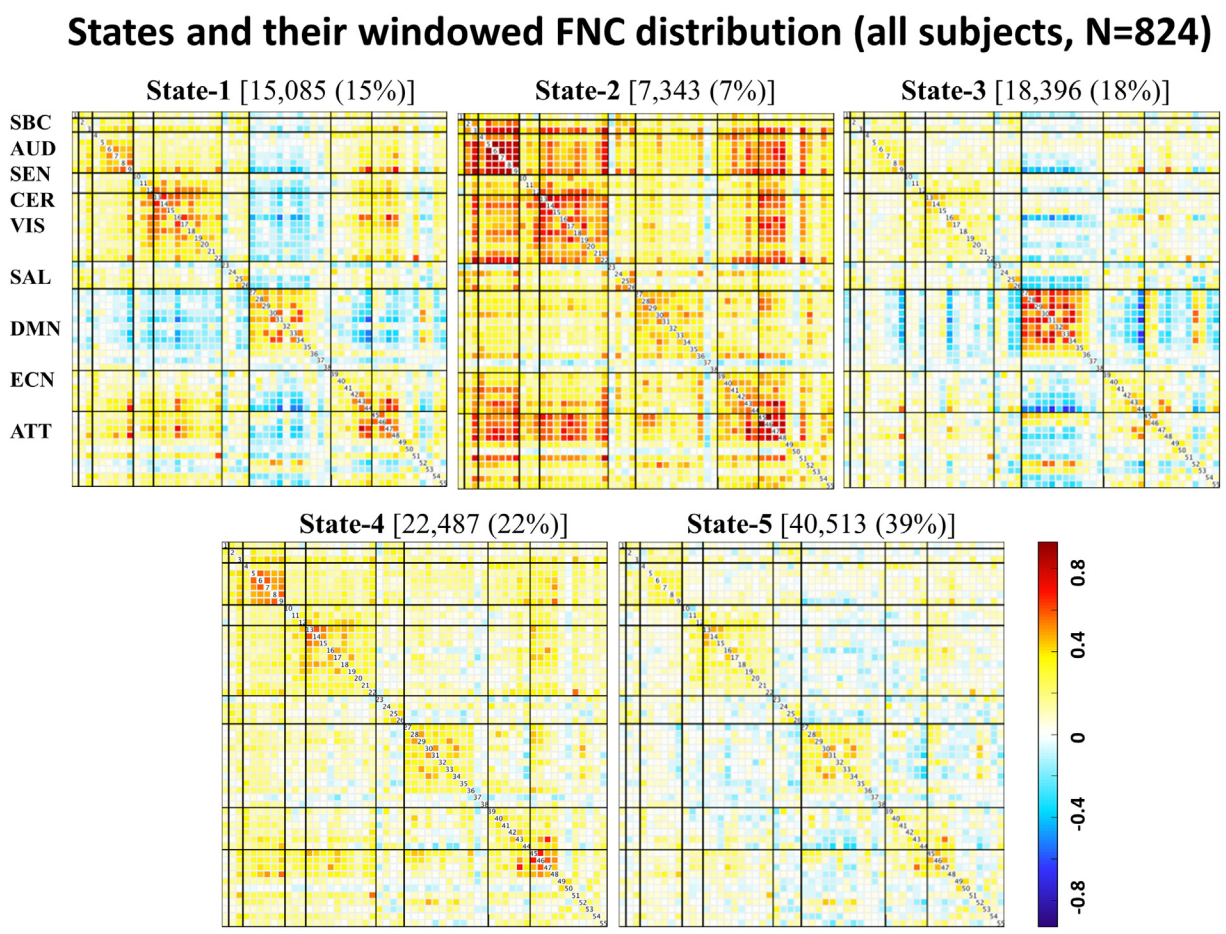

Fig. 2. States 1–5 functional network connectivity (FNC) matrices showing all pairwise correlations between RSNs grouped into nine functional domains [subcortical (SBC), auditory (AUD), sensorimotor (SEN), cerebellar (CER), visual (VIS), salience (SAL), default mode network (DMN), executive control (ECN), attentional (ATT)]. Positive correlations are in the yellow to red range, while negative correlations are light to dark blue.

2018. It is important to recognize the functional roles of effective nodes in the context of known symptomatology constitutive of psychopathy – including poor behavioral control, impulsiveness, and poor integration of affective information into ongoing behavior management and planning (Hamilton et al., 2015; Hare, 2003). The functional roles of nodes in these effects suggest that brain areas contributing to networks of attentional control and salience (e.g. amygdala, insula) are not well integrated with brain areas contributing to networks governing extended processes like perception of the environment, strategic planning, and behavioral execution (occipital, sensorimotor, supplementary motor cortex) (Amaral et al., 2003; Anderson et al., 2017; Espinoza et al., 2018).

While several associations with Factor 1 scores were negative, some positive associations were also observed. Connectivity between the precuneus (attentional domain) and subcortical structures including the putamen was higher for those with elevated Factor 1 psychopathy scores, and this pattern may further reinforce functional abnormalities promoting impaired attentive processes. The precuneus is part of the default mode network, highly active during rest and mind-wandering, and the putamen is important in attention, alerting, and orienting toward salient, motivationally relevant cues. Ordinarily, these networks will show anticorrelated patterns of activity, demonstrating a functional decoupling between these systems. A relative increase in connectivity strength between these elements (in those with elevated Factor 1 scores) may indicate weaker decoupling of these areas, and impaired efficiency in (re)directing attention. Indeed deficits in attention switching, automatic attention capture are features of attention-based models of psychopathy (Newman et al., 2010). Previous studies in fMRI have confirmed abnormal coupling between DMN and other networks (Anderson et al., 2018). Further, studies examining attentional abnormalities in those with ADHD have also noted abnormalities in functional connectivity between precuneus-putamen, described as decreased inverse connectivity between DMN and putamen (Cao et al., 2009; Posner et al., 2014). These findings are thus interpretable in accord with theoretical models of impaired attentional mechanisms in psychopathy as well as empirical observations in other pathological manifestations of attentional abnormalities.

The interpersonal/affective features of psychopathy (Factor 1) were also associated with increased mean dwell time in State-5 – a pattern of widespread loose functional connectivity across nodes of the brain. This relatively increased dwell time in a state not punctuated by strong anatomically segregated signals may reflect lagging or inefficient transfer of information between disparate functional nodes. This is also reflected in the low number of transitions across the time domain that accompanied high scores on these same features (Factor 1) of psychopathy. By contrast, Factor 2 elements – behavioral/lifestyle features of psychopathy – were associated with the opposite pattern, namely, relatively more frequent transitions. These patterns of results are thus consistent with known cognitive-attentive features of psychopathy, and with other examples of pathology in attentive processes.

Discriminating unique—and even opposing—physiological effects associated with the different factors of psychopathy has been an important emerging trend in recent related clinical neuroscience research. Importantly, Factor 2 elements, considered apart from Factor 1, represent a reduced set of features relatively more common among highly antisocial populations, like the present one. Psychophysiological effects

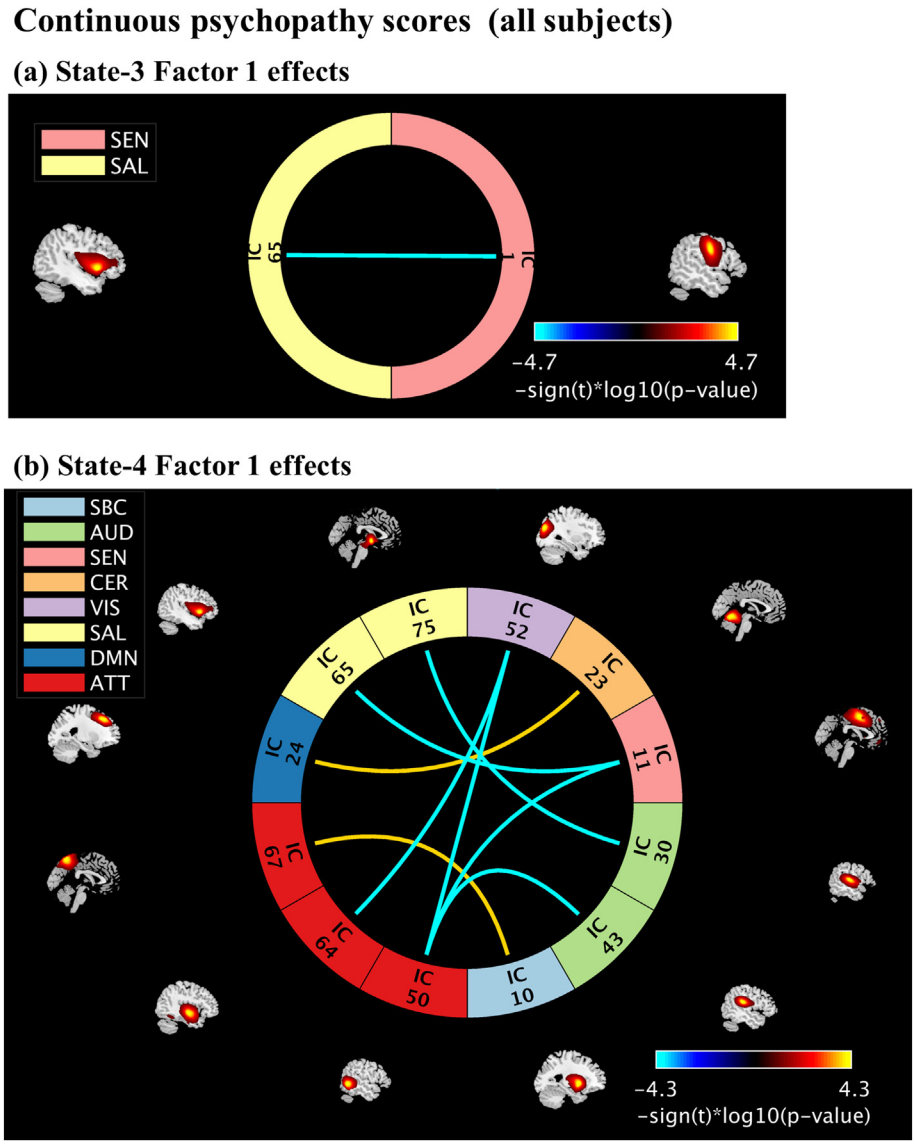

Fig. 3. Continuous psychopathy score effects on States FNC. Results are displayed as - sign(t)*log10(*p*-value) and include only the *p*-values that survived FDR correction. Positive correlations are in the yellow to red range, while negative correlations are light to dark blue. Independent components (ICs) name descriptions are listed in Table 3.

associated specifically with Factor 2, alone, may reflect more generic patterns associated with more prevalent manifestations of antisocial behavior, whereas patterns associated with Factor 1 elements may reflect a separate pathophysiology more discriminative of the unique (personality) features that set psychopaths apart in a large population of offenders. Indeed, distinct and even opposite neurological effects have been often previously been noted in connectivity studies by examining these factors separately, reflecting the importance of Factor 1 features for characterizing psychopathy (Espinoza et al., 2018; Juarez et al., 2013; Wolf et al., 2015; Philippi et al., 2015).

Finally, when examining discrete groups – specifically comparing those meeting full clinical characteristics of psychopathy with those selected for low representative symptoms—patterns in State-5 exhibited low connectivity between amygdala and bilateral lingual gyrus and superior occipital – parts of the visual processing stream. The amygdala notably plays a role in amplifying signal (through feedback loops) involved in visual processing for emotionally laden images, thus prioritizing vitally important information in early perceptual processes (Amaral et al., 2003; Pessoa and Ungerleider, 2004; Vuilleumier, 2005). Prior work has noted specific deficits in this amygdala-mediated enhancement of signal in the visual cortex, related to Factor 1 elements of psychopathy, and it was speculated that disrupted connectivity between amygdala and visual processing streams may be responsible (Anderson et al., 2017). The present work confirms disrupted connectivity between amygdala and parts of the visual stream, particularly in dynamic shifts of functional activity represented in State-5 of this analysis. This also reiterates the importance of examining dynamic states, as relevant differences in functional connectivity might otherwise be obscured by quantifying only static connectivity collapsed across the time domain. In combination with prior work (Espinoza et al., 2018; Anderson et al., 2018), this may be indicative of at least one mechanism by which appropriate integration of emotional information is interfered with in psychopathy.

Putting the present findings in the context of contemporary neurocognitive models of psychopathy, only very recent attention has been paid to formal network properties and their abnormal associations. This does not negate prior models which are still informative. For instance, psychopathy has long been associated with specific deficits in emotional processing and attention, and such deficits may be attributed to failures in neural systems that include salience network and attention

Table 3
Summary results of all states FNC pairs showing psychopathy associations' Continuous psychopathy scores (all subjects, N = 824), and discrete psychopathy scores [Non-PSY Group-1 (PCL-R ≤ 15, N = 159), PSY Group-2 (PCL-R ≥ 30)].

RSNs pairs	Domains	Beta	p-Value
Continuous psychopathy scores (all subjects)			
State-3, factor 1 effects			
IC65-IC1: insula* – precentral gyrus	SAL-SEN	−0.0181	1.84e-05
State-4, factor 1 effects			
IC75-IC30: amygdala* – superior temporal gyrus	SAL-AUD	−0.0140	1.30e-04
IC65-IC11: insula* – supplementary motor area	SAL-SEN	−0.0149	5.25e-05
IC24-IC23: middle frontal gyrus - cerebellum	DMN-CER	0.0136	1.67e-04
IC67-IC10: precuneus - putamen	ATT-SBC	0.0134	1.40e-04
IC64-IC52: superior temporal gyrus – superior occipital gyrus	ATT-VIS	−0.0140	6.50e-05
IC50-IC43: middle temporal gyrus – postcentral gyrus	ATT-AUD	−0.0134	9.81e-05
IC50-IC11: middle temporal gyrus – supplementary motor area	ATT-SEN	−0.0147	6.38e-05
IC50-IC52: middle temporal gyrus – superior occipital gyrus	ATT-VIS	−0.0150	1.03e-04
Discrete psychopathy scores (non-PSY and PSY)			
State-5, PCL-R effects			
IC75-IC20: Amygdala* – right lingual gyrus	SAL-VIS	−0.1469	8.87e-06
IC75-IC48: Amygdala* – left lingual gyrus	SAL-VIS	−0.1424	9.04e-06
IC75-IC52: Amygdala* – superior occipital gyrus	SAL-VIS	−0.1190	5.96e-05

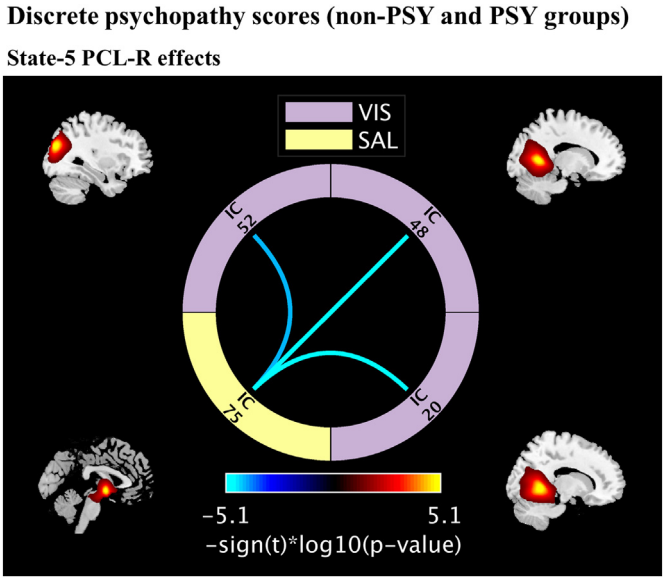

Fig. 4. Discrete psychopathy trait effects on states FNC. Results are displayed as - sign(t)*log10(p-value) and include only the p-values that survived FDR correction. Positive correlations are in the yellow to red range, while negative correlations are light to dark blue. Independent components (ICs) name descriptions are listed in Table 3.

networks (Anderson et al., 2018; Anderson et al., 2017; Newman et al., 2010).A more recent model has formally extended these ideas in a model that addresses impaired integration across large scale intrinsic networks in the brain (Hamilton et al., 2015). The present results align with such suggestions, and offer new evidence exhibiting the disrupted networks in real time. The methods in this study represent a valuable departure from traditional task-based functional MRI investigations by measuring fluctuating connectivity patterns at rest. This eliminates any task-specific limitations that inevitably accompany traditional fMRI designs, and highlights variation in signal that accompanies intrinsic connectivity, independent of specific task demands. The present findings also advance beyond traditional static functional connectivity studies by demonstrating where and when these disruptions in connectivity arise across limited states of connectivity. The present findings are indeed the first reported confirmation that dynamic states of network connectivity are measurably disrupted, both in categorically-defined psychopaths, and in measurable association with elemental psychopathic personality traits. In addition, by exploring FNC in the whole-brain we identified a total of thirteen non-paralimbic RSNs from nine functional domains (subcortical, auditory, sensorimotor, cerebellar, visual, salience, default mode network, executive control and attentional) related to psychopathy, implying that these effects may exert influences over networks outside primary limbic and paralimbic regions.

4.1. Study limitations

There are a number of limitations to consider in this study. First, because this was a resting-state fMRI study it is not straightforward to attribute the observed effects to specific functional domains without engaging in reverse inference. Studies which combine extended rest and task data are needed to address this point (Cetin et al., 2014). In addition, because association between psychopathy traits and dynamic functional network connectivity was limited to a forensic population it is difficult to determine whether the results would be the same for individuals who score high on psychopathy but were not incarcerated. Relatedly, while incarcerated populations undergo enforced abstinence from drug use while in prison (i.e. acute effects of drug use are limited), they also typically exhibit high rates of (prior) substance abuse history, which may also impact connectivity measures. Typically, substance abuse is more closely related to Factor 2 (lifestyle/behavioral) elements of psychopathy, which did not show significant effects in our connectivity analyses. In future work, we plan to examine substance use disorder measures and associations to psychopathy more directly. Finally, the sliding window approach requires a window size selection. The selected size should be able to capture functional connectivity variability in small time domains (Sakoglu et al., 2010). Based on this validated recommendation, in this study, we selected a window size of 15 TRs (30 s). It will be interesting to examine variability in time-varying FNC for different window lengths, compare results with other approaches such as the time-frequency analysis (Yaesoubi et al., 2015), measure functional connectivity using higher order statistic such as mutual information (Gomez-Verdejo et al., 2012).

5. Conclusion

The results from the current study are in agreement with previous work that found RSNs from paralimbic regions (amygdala and insula) related to psychopathy. In addition, by exploring FNC in the whole-brain we identified a total of 13 non-paralimbic RSNS from nine functional domains (subcortical, auditory, sensorimotor, cerebellar, visual, salience, default mode network, executive control and attentional) related to psychopathy. We also showed that individuals with higher Factor 1 scores (emotional and interpersonal relationships) spend more time in State-5 (a state with weaker connectivity overall), and changed state less frequently compared to those with lower scores. On the other hand, individuals with higher Factor 2 scores (impulsive and antisocial behaviors) showed more dynamism (changes to and from different states) than those with lower scores. Our results did not reveal within-states FNC associations with Factor 2 scores, nor did they reveal any associations between dynamism (clustering measure) and total PCL-R scores.

Acknowledgments

This work was supported by grants from the National Institutes of Health (R01NS054893, P20GM103472, R01EB020407, R01DA026964, R01MH090169, R01MH087525, R01DA026505, R01DA020870, R01MH070539, R01MH114028, R01MH109329, R01AA026290, P30GM122734), the National Science Foundation (1539067).

Declaration of Competing Interest

No competing financial interest exists.

References

Allen, E.A., Erhardt, E.B., Damaraju, E., Gruner, W., Segall, J.M., Silva, R.F., Havlicek, M., Rachakonda, S., Fries, J., Kalyanam, R., Michael, A.M., Caprihan, A., Turner, J.A., Eichele, T., Adelsheim, S., Bryan, A.D., Bustillo, J., Clark, V.P., Feldstein Ewing, S.W., Filbey, F., Ford, C.C., Hutchison, K., Jung, R.E., Kiehl, K.A., Kodituwakku, P., Komesu, Y.M., Mayer, A.R., Pearlson, G.D., Phillips, J.P., Sadek, J.R., Stevens, M., Teuscher, U., Thoma, R.J., Calhoun, V.D., 2011. A baseline for the multivariate comparison of resting-state networks. Front. Syst. Neurosci. 5, 2.

Allen, E.A., Damaraju, E., Plis, S.M., Erhardt, E.B., Eichele, T., Calhoun, V.D., 2014. Tracking whole-brain connectivity dynamics in the resting state. Cereb. Cortex (New York, N.Y.: 1991) 24, 663–676.

Amaral, D.G., Behniea, H., Kelly, J.L., 2003. Topographic organization of projections from the amygdala to the visual cortex in the macaque monkey. Neuroscience 118, 1099–1120.

Anderson, N.E., Kiehl, K.A., 2012. The psychopath magnetized: insights from brain imaging. Trends Cogn. Sci. 16, 52–60.

Anderson, N.E., Steele, V.R., Maurer, J.M., Rao, V., Koenigs, M.R., Decety, J., Kosson, D.S., Calhoun, V.D., Kiehl, K.A., 2017. Differentiating emotional processing and attention in psychopathy with functional neuroimaging. Cogn. Affect. Behav. Neurosci. 17, 491–515.

Anderson, N.E., Maurer, J.M., Steele, V.R., Kiehl, K.A., 2018. Psychopathic traits associated with abnormal hemodynamic activity in salience and default mode networks during auditory oddball task. Cogn. Affect. Behav. Neurosci. 18, 564–580.

Blair, R.J., 2008. The amygdala and ventromedial prefrontal cortex: functional contributions and dysfunction in psychopathy. Philos. Trans. R. Soc. Lond. Ser. B Biol. Sci. 363, 2557–2565.

Calhoun, V.D., Adali, T., Pearlson, G.D., Pekar, J.J., 2001. A method for making group inferences from functional MRI data using independent component analysis. Hum. Brain Mapp. 14, 140–151.

Calhoun, Vince D., Miller, R., Pearlson, G., Adalı, T., 2014. The chronnectome: time-varying connectivity networks as the next frontier in fMRI data discovery. Neuron 84, 262–274.

Cao, X., Cao, Q., Long, X., Sun, L., Sui, M., Zhu, C., Zuo, X., Zang, Y., Wang, Y., 2009. Abnormal resting-state functional connectivity patterns of the putamen in medication-naive children with attention deficit hyperactivity disorder. Brain Res. 1303, 195–206.

Cetin, M.S., Christensen, F., Abbott, C.C., Stephen, J.M., Mayer, A.R., Canive, J.M., Bustillo, J.R., Pearlson, G.D., Calhoun, V.D., 2014. Thalamus and posterior temporal lobe show greater inter-network connectivity at rest and across sensory paradigms in schizophrenia. NeuroImage 97, 117–126.

Erhardt, E.B., Rachakonda, S., Bedrick, E.J., Allen, E.A., Adali, T., Calhoun, V.D., 2011. Comparison of multi-subject ICA methods for analysis of fMRI data. Hum. Brain Mapp. 32, 2075–2095.

Ermer, E., Cope, L.M., Nyalakanti, P.K., Calhoun, V.D., Kiehl, K.A., 2012. Aberrant paralimbic gray matter in criminal psychopathy. J. Abnorm. Psychol. 121, 649–658.

Espinoza, F.A., Vergara, V.M., Reyes, D., Anderson, N.E., Harenski, C.L., Decety, J., Rachakonda, S., Damaraju, E., Rashid, B., Miller, R.L., Koenigs, M., Kosson, D.S., Harenski, K., Kiehl, K.A., Calhoun, V.D., 2018. Aberrant functional network connectivity in psychopathy from a large (N = 985) forensic sample. Hum. Brain Mapp. 39, 2624–2634.

Friedman, J., Hastie, T., Tibshirani, R., 2008. Sparse inverse covariance estimation with the graphical lasso. Biostatistics (Oxford, England) 9, 432–441.

Friston, K.J., Holmes, A.P., Worsley, K.J., Poline, J.P., Frith, C.D., Frackowiak, R.S.J., 1994. Statistical parametric maps in functional imaging: a general linear approach. Hum. Brain Mapp. 2, 189–210.

Gao, Y., Glenn, A.L., Schug, R.A., Yang, Y., Raine, A., 2009. The neurobiology of psychopathy: a neurodevelopmental perspective. Can. J. Psychiatr. 54, 813–823.

Gomez-Verdejo, V., Martinez-Ramon, M., Florensa-Vila, J., Oliviero, A., 2012. Analysis of fMRI time series with mutual information. Med. Image Anal. 16, 451–458.

Hamilton, R.K., Hiatt Racer, K., Newman, J.P., 2015. Impaired integration in psychopathy: a unified theory of psychopathic dysfunction. Psychol. Rev. 122, 770–791.

Hare, R.D., 1991. Manual for the Hare Psychopathy Checklist-Revised. Toronto. Multi-Health Systems.

Hare, R.D., 2003. Manual for the Hare Psychopathy Checklist-revised, 2nd ed. Multi-Health Systems, Toronto.

Hare, R.D., Neumann, C.S., 2005. Structural models of psychopathy. Curr. Psychiatry Rep. 7, 57–64.

Hare, R.D., Neumann, C.S., 2010. Psychopathy: assessment and forensic implications. In: Responsibility and Psychopathy: Interfacing Law, Psychiatry and Philosophy, pp. 93–123.

Harpur, T.J., Hare, R.D., Hakstian, A.R., 1989. Two-factor conceptualization of psychopathy: construct validity and assessment implications. Psychol. Assess. 1, 6.

Hemphill, J.F., Hare, R.D., Wong, S., 1998. Psychopathy and recidivism: a review. Leg. Criminol. Psychol. 3, 139–170.

Hiser, J., Koenigs, M., 2018. The multifaceted role of the ventromedial prefrontal cortex in emotion, decision making, social cognition, and psychopathology. Biol. Psychiatry 83, 638–647.

Hoppenbrouwers, S.S., Nazeri, A., de Jesus, D.R., Stirpe, T., Felsky, D., Schutter, D.J., Daskalakis, Z.J., Voineskos, A.N., 2013. White matter deficits in psychopathic offenders and correlation with factor structure. PLoS One 8, e72375.

Hutchison, R.M., Womelsdorf, T., Allen, E.A., Bandettini, P.A., Calhoun, V.D., Corbetta, M., Della Penna, S., Duyn, J.H., Glover, G.H., Gonzalez-Castillo, J., Handwerker, D.A., Keilholz, S., Kiviniemi, V., Leopold, D.A., de Pasquale, F., Sporns, O., Walter, M., Chang, C., 2013. Dynamic functional connectivity: promise, issues, and interpretations. NeuroImage 80, 360–378.

Juarez, M., Kiehl, K.A., Calhoun, V.D., 2013. Intrinsic limbic and paralimbic networks are associated with criminal psychopathy. Hum. Brain Mapp. 34, 1921–1930.

Kiehl, K.A., 2006. A cognitive neuroscience perspective on psychopathy: evidence for paralimbic system dysfunction. Psychiatry Res. 142, 107–128.

Korponay, C., Pujara, M., Deming, P., Philippi, C., Decety, J., Kosson, D.S., Kiehl, K.A., Koenigs, M., 2017a. Impulsive-antisocial dimension of psychopathy linked to enlargement and abnormal functional connectivity of the striatum. Biol. Psychiatry 2, 149–157.

Korponay, C., Pujara, M., Deming, P., Philippi, C., Decety, J., Kosson, D.S., Kiehl, K.A., Koenigs, M., 2017b. Impulsive-antisocial psychopathic traits linked to increased volume and functional connectivity within prefrontal cortex. Soc. Cogn. Affect. Neurosci. 12, 1169–1178.

Meda, S.A., Giuliani, N.R., Calhoun, V.D., Jagannathan, K., Schretlen, D.J., Pulver, A., Cascella, N., Keshavan, M., Kates, W., Buchanan, R., Sharma, T., Pearlson, G.D., 2008. A large scale (N = 400) investigation of gray matter differences in schizophrenia using optimized voxel-based morphometry. Schizophr. Res. 101, 95–105.

Motzkin, J.C., Newman, J.P., Kiehl, K.A., Koenigs, M., 2011. Reduced prefrontal connectivity in psychopathy. J. Neurosci. 31, 17348–17357.

Newman, J.P., 1998. Psychopathic behavior: An information processing perspective. In: Cooke, D.J., Hare, R.D., Forth, A. (Eds.), Psychopathy: Theory, Research and Implications for Society. vol. 88. Kluwer Academic Publishers, Dordrecht, The Netherlands, pp. 81–104.

Newman, J.P., Curtin, J.J., Bertsch, J.D., Baskin-Sommers, A.R., 2010. Attention moderates the fearlessness of psychopathic offenders. Biol. Psychiatry 67, 66–70.

Pessoa, L., Ungerleider, L.G., 2004. Neuroimaging studies of attention and the processing of emotion-laden stimuli. Prog. Brain Res. 144, 171–182.

Philippi, C.L., Pujara, M.S., Motzkin, J.C., Newman, J., Kiehl, K.A., Koenigs, M., 2015. Altered resting-state functional connectivity in cortical networks in psychopathy. J. Neurosci. 35, 6068–6078.

Posner, J., Park, C., Wang, Z., 2014. Connecting the dots: a review of resting connectivity MRI studies in attention-deficit/hyperactivity disorder. Neuropsychol. Rev. 24, 3–15.

Power, J.D., Barnes, K.A., Snyder, A.Z., Schlaggar, B.L., Petersen, S.E., 2012. Spurious but systematic correlations in functional connectivity MRI networks arise from subject motion. NeuroImage 59, 2142–2154.

Rachakonda, S., Silva, R.F., Liu, J., Calhoun, V.D., 2016. Memory efficient PCA methods for large group ICA. Front. Neurosci. 10.

Raine, A., Lencz, T., Taylor, K., Hellige, J.B., Bihrle, S., Lacasse, L., Lee, M., Ishikawa, S., Colletti, P., 2003. Corpus callosum abnormalities in psychopathic antisocial individuals. Arch. Gen. Psychiatry 60, 1134–1142.

Robinson, S., Basso, G., Soldati, N., Sailer, U., Jovicich, J., Bruzzone, L., Kryspin-Exner, I., Bauer, H., Moser, E., 2009. A resting state network in the motor control circuit of the basal ganglia. BMC Neurosci. 10, 137.

Sakoglu, U., Pearlson, G.D., Kiehl, K.A., Wang, Y.M., Michael, A.M., Calhoun, V.D., 2010. A method for evaluating dynamic functional network connectivity and task-modulation: application to schizophrenia. Magma (New York, N.Y.) 23, 351–366.

Smith, S.M., Fox, P.T., Miller, K.L., Glahn, D.C., Fox, P.M., Mackay, C.E., Filippini, N., Watkins, K.E., Toro, R., Laird, A.R., Beckmann, C.F., 2009. Correspondence of the brain's functional architecture during activation and rest. Proc. Natl. Acad. Sci. U. S. A 106, 13040–13045.

Smith, S.M., Miller, K.L., Salimi-Khorshidi, G., Webster, M., Beckmann, C.F., Nichols, T.E., Ramsey, J.D., Woolrich, M.W., 2011. Network modelling methods for FMRI. NeuroImage 54, 875–891.

Vuilleumier, P., 2005. How brains beware: neural mechanisms of emotional attention. Trends Cogn. Sci. 9, 585–594.

Wolf, R.C., Pujara, M.S., Motzkin, J.C., Newman, J.P., Kiehl, K.A., Decety, J., Kosson, D.S., Koenigs, M., 2015. Interpersonal traits of psychopathy linked to reduced integrity of the uncinate fasciculus. Hum. Brain Mapp. 36, 4202–4209.

Yaesoubi, M., Allen, E.A., Miller, R.L., Calhoun, V.D., 2015. Dynamic coherence analysis of resting fMRI data to jointly capture state-based phase, frequency, and time-domain information. NeuroImage 120, 133–142.

Yoder, K.J., Porges, E.C., Decety, J., 2015. Amygdala subnuclei connectivity in response to violence reveals unique influences of individual differences in psychopathic traits in a nonforensic sample. Hum. Brain Mapp. 36, 1417–1428.